A Letters Journal Exploring
the Frontiers of Physics

OFFPRINT

Capillary rise between flexible walls

T. Cambau, J. Bico and E. Reyssat

EPL, **96** (2011) 24001

IMPACT FACTOR

2.753*

* As listed in the ISI® 2010 Science Citation Index Journal Citation Reports

OVER

500 000

full text downloads in 2010

30 DAYS

average receipt to online publication in 2010

16 961

citations in 2010
37% increase from 2007

"We've had a very positive experience with EPL, and not only on this occasion. The fact that one can identify an appropriate editor, and the editor is an active scientist in the field, makes a huge difference."

Dr. Ivar Martinv
Los Alamos National Laboratory, USA

Six good reasons to publish with EPL

We want to work with you to help gain recognition for your high-quality work through worldwide visibility and high citations.

1. **Quality** – The 40+ Co-Editors, who are experts in their fields, oversee the entire peer-review process, from selection of the referees to making all final acceptance decisions

2. **Impact Factor** – The 2010 Impact Factor is 2.753; your work will be in the right place to be cited by your peers

3. **Speed of processing** – We aim to provide you with a quick and efficient service; the median time from acceptance to online publication is 30 days

4. **High visibility** – All articles are free to read for 30 days from online publication date

5. **International reach** – Over 2,000 institutions have access to EPL, enabling your work to be read by your peers in 100 countries

6. **Open Access** – Articles are offered open access for a one-off author payment

Details on preparing, submitting and tracking the progress of your manuscript from submission to acceptance are available on the EPL submission website **www.epletters.net**.

If you would like further information about our author service or EPL in general, please visit **www.epljournal.org** or e-mail us at **info@epljournal.org**.

EPL is published in partnership with:

European Physical Society | Società Italiana di Fisica | EDP Sciences | IOP Publishing

A LETTERS JOURNAL EXPLORING THE FRONTIERS OF PHYSICS

October 2011

EPL, **96** (2011) 24001
doi: 10.1209/0295-5075/96/24001

www.epljournal.org

Capillary rise between flexible walls

T. CAMBAU, J. BICO and E. REYSSAT[(a)]

Physique et Mécanique des Milieux Hétérogènes, UMR CNRS 7636, ESPCI-ParisTech, Paris Diderot University 10 rue Vauquelin, 75005 Paris, France, EU

received 28 April 2011; accepted in final form 29 August 2011
published online 29 September 2011

PACS 47.56.+r – Flows through porous media
PACS 46.70.De – Beams, plates, and shells
PACS 47.55.N- – Interfacial flows

Abstract – We report experimental work on capillary rise of a liquid in a cell formed by parallel plates, one of which is flexible. We show that above a critical width, the cell collapses under the negative capillary pressure in the liquid. This collapse allows the liquid to rise virtually without limit between the plates. The height of the rising front is found to increase with time as $t^{1/3}$, a characteristic of capillary imbibition in a wedge.

Introduction. – When dipped into coffee, a sugar cube absorbs the liquid owing to capillary forces. The very general phenomenon of capillary imbibition occurs as soon as a porous medium is put in contact with a wetting liquid and has important consequences for human, animal and plant lives, from soil sciences and oil extraction [1,2], to construction materials [3], food and paper industries [4,5], the stability of micro-mechanical systems [6], feeding of birds [7] or the rise of sap in trees [8].

The equilibrium height and wicking dynamics of a wetting liquid front rising in a porous medium are both widely documented in textbooks [9]. The equilibrium height h_e of a liquid column in a circular capillary tube was long observed to be inversely proportional to the radius r of the tube. This result, experimentally demonstrated in the 18th century and commonly known as Jurin's law, was first explained by Laplace [10]. For a totally wetting liquid, h_e is set by a balance of the capillary pressure $2\gamma/r$ with the hydrostatic pressure $\rho g h_e$, which yields

$$h_e = \frac{2\gamma}{\rho g r}, \tag{1}$$

where γ and ρ stand for the surface tension and the density of the liquid and g for the gravitational acceleration. Note that eq. (1) holds for r much smaller than the capillary length $\sqrt{\gamma/\rho g}$.

The basic dynamical law for the rise of liquid in a tube is commonly referred to as Washburn's law. It describes the progression of the liquid front far from equilibrium and states that the penetration length $h(t)$ of liquid in the tube behaves pseudo-diffusively

$$h(t) = \sqrt{\mathcal{D}t}, \quad \mathcal{D} = \frac{2\gamma r}{\eta}, \tag{2}$$

where η is the viscosity of the liquid. Equation (2) remains valid until h approaches the equilibrium height h_e within a characteristic time scale τ given by $h_e \sim \sqrt{\mathcal{D}\tau}$

$$\tau \sim \frac{\eta \rho g}{\gamma^2} h_e^3. \tag{3}$$

These results were derived in the early 1900s by Bell and Cameron [11], Lucas [12] and Washburn [13], motivated by separation, soil sciences and oil extraction.

Equations (1) and (2) have proven very general and robust, and describe the capillary transport in many complex and disordered porous media with typical pore size r. Yet, in a number of cases, these laws do not hold any longer. The reasons for discrepancies are various: inertial effects [14], evaporation, surfactants, contact angles, geometrical singularities and heterogeneities in the pore network. More particularly, deformations of the porous matrix may occur as the liquid penetrates inside the material. Microfluidic channels closed with thin flexible walls can indeed collapse under negative capillary pressures as nicely shown by van Honschoten *et al.* [15–17]. The possible collapse of nanotubes partially filled with a liquid droplet has also been predicted numerically [18]. More dramatically, a similar collapse may also occur in the lung airways of premature infants with fatal consequences [19–21]. Model experiments allow to extract the physical ingredients involved in complex nanoscale

(a) E-mail: etienne.reyssat@normalesup.org

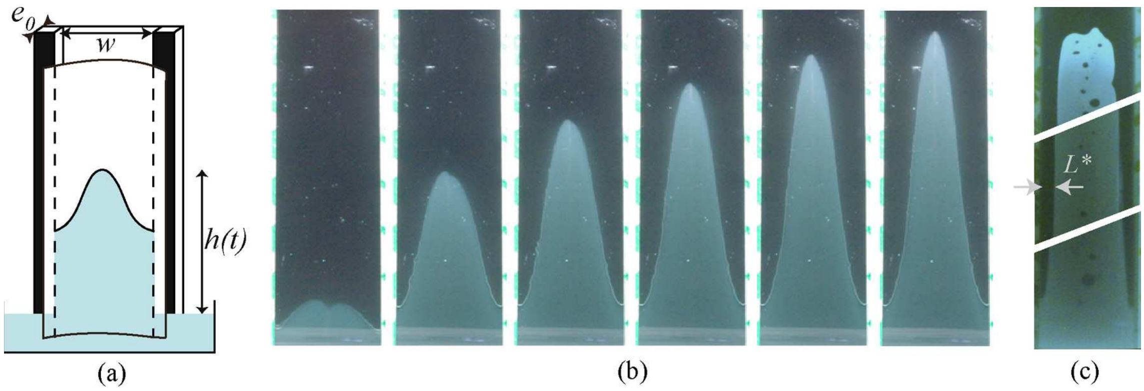

Fig. 1: (Colour on-line) (a) Experimental setup: a flexible polymer membrane (white) is separated from a rigid plate of width w by spacers of thickness e_0. The flexible wall is simply supported on the spacers and the cell is very slightly tilted with respect to the vertical direction to prevent the flexible wall from falling. (b) Owing to capillary forces, the liquid rises between the plates and forms a liquid finger. $w = 5$ cm and the snapshots are taken every 70 s. (c) Shape of the front at very long times. A dry region of width L^* develops along the spacers. The picture is cut in three parts as its actual height is approximately three times that of the pictures in panel (b) of this figure.

or biological systems. In particular, recent works address the problem of capillary rise in a wedge [22] or between flexible lamella [23–25]. In this paper, we focus on a novel experiment which combines both a geometrical singularity and deformability.

Capillary rise between elastic plates: statics. – We consider the capillary rise between two vertical plates of width w, separated along the vertical edges by a pair of spacers of thickness e_0 (fig. 1(a)). One of the plates is a thick rigid glass plate, while the other one is a flexible polymer film that is simply supported on the spacers. The lower part of the imbibition cell is put in contact with a bath of wetting liquid, typically silicon oil. We monitor the liquid front that rises owing to capillary forces. In the case of a rigid cell, a horizontal wetting front follows Washburn dynamics and quickly saturates to the Jurin height prescribed by the cell thickness e_0: $h_e = 2\gamma/\rho g e_0$. For silicon oil of viscosity 15 mPa s, density $\rho = 950\,\mathrm{kg\,m^{-3}}$ and surface tension $\gamma = 21\,\mathrm{mN/m}$ in a cell of thickness $e_0 = 330\,\mu\mathrm{m}$, the rise stops at 14 mm after roughly 10 s. In a flexible cell the phenomenology is very different. As shown in fig. 1(b), a liquid finger rises at the center of the cell, while a small region along the spacers remains dry. At long times (fig. 1(c)), the width of the dry region does not depend on altitude z any more, except close to the rising front. Reaching 140 mm after 1000 s, the height h of the front does not seem to saturate (fig. 2). In practice, the finite size of the cell eventually limits the rise.

We first address the statics of these systems, and describe the shape of the flexible wall. The liquid rising between the plates exerts a negative pressure on the walls of the cell which thus tends to collapse. Using the fringe projection technique described in [26], we measure the thickness profile of the imbibed cell (fig. 3): in the central wet region, the flexible membrane is almost flat and contacts the rigid wall.

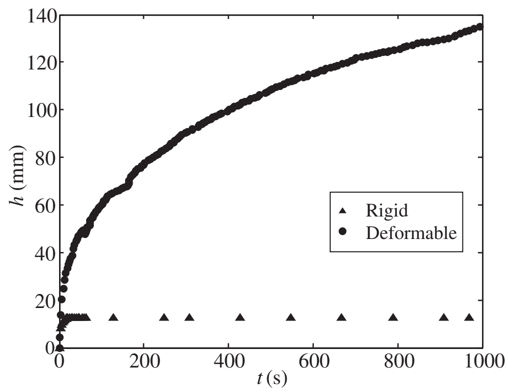

Fig. 2: Height $h(t)$ of the imbibition front as a function of time in a cell of thickness $e_0 = 330\,\mu\mathrm{m}$, for silicon oil of viscosity $\eta = 15.4$ mPa s, surface tension $\gamma = 21$ mN/m and density $\rho = 950\,\mathrm{kg\,m^{-3}}$. In a rigid cell (triangles), $h(t)$ saturates within a few seconds at the Jurin height $h_e \simeq 13$ mm. In a flexible cell (circles), the contact between opposite walls enables the liquid to virtually rise to infinity. After 1000 s, the liquid front reaches 140 mm and does not saturate.

Close to the sides, the walls gradually separate and form a wedge, whose thickness reaches e_0 at the spacers (fig. 3(b)). The infinitesimal spacing available in this self-generated corner enables the liquid to virtually rise to infinite heights. We note that, at long times, the width L^* of the dry deformed domain does not change with height. Far from the tip, the section of the collapsed wall is thus almost invariant by translation along the vertical axis (fig. 1(c)). The extension of the void region results from a competition between capillary adhesion that tends to bring the walls in contact and the counterbalancing stiffness of the sheet. Indeed, the adhesion of the flexible wall over a length L would lead to a gain in surface energy $E_\gamma = 2\gamma L$ per unit height (we assume that the liquid totally wets the walls). This gain is however reduced by

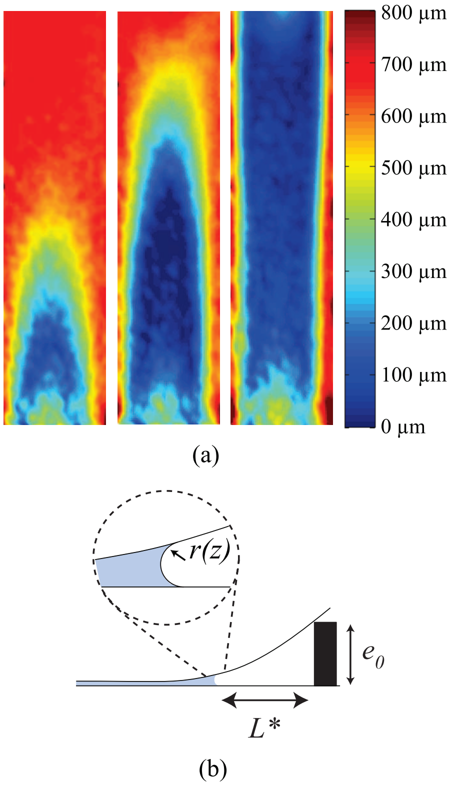

Fig. 3: (Colour on-line) (a) Thickness maps of the cell measured with the fringe projection technique described in [26]. The maps were taken at $t=15\,\mathrm{s}$, $200\,\mathrm{s}$ and $1200\,\mathrm{s}$. At long times, the center of the cell is flat, while a dry region of width L^* close to the spacers forms a wedge. The vertex of this corner is filled with a liquid meniscus. The width of the cell is 40 mm. (b) Schematic horizontal section of the cell at long times.

the cost in elastic energy corresponding to the deformation of the flexible wall. In the region where the section is invariant by translation, the wall is simply bent and the bending energy per unit area stored in this process is of order $B\kappa^2$, where B and κ are the bending modulus and curvature of the elastic membrane. In terms of scaling, B is proportional to $E\delta^3$, where E and δ are the Young modulus and thickness of the wall, and κ scales as e_0/L^2, where L is the length of the wedge. Taking all numerical factors into account (within the limit of small deformations), the elastic energy $\mathcal{E}_B$ stored per unit height of the cell reads [23]

$$\mathcal{E}_B = \frac{3}{2}\frac{B{e_0}^2}{L^3}. \qquad (4)$$

The total energy stored in one wedge is finally given by

$$\mathcal{E} = \mathcal{E}_B + \mathcal{E}_\gamma = \frac{3}{2}\frac{B{e_0}^2}{L^3} + 2\gamma L. \qquad (5)$$

The selected length L^* minimizes $\mathcal{E}$, which leads to

$$L^* = \left(\frac{9B{e_0}^2}{4\gamma}\right)^{1/4} \simeq 1.22\sqrt{e_0 L_{ec}}, \qquad (6)$$

where $L_{ec} = \sqrt{B/\gamma}$ is the elastocapillary length of the system [27]. This prediction for L^* is in quantitative agreement with our experiments (fig. 4(a)). The determination of L^* provides a criterion for the flexible character of the cell wall. Indeed, the wall is expected to collapse only if $w > 2L^*$. In this situation wedges are formed and allow the liquid to rise indefinitely. Otherwise the flexible wall deflects as described in [16], but not enough to collapse. Figure 4(b) shows a phase diagram summarizing these different regimes. Cells with a width $w < 2L^*$ are not able to convey the liquid to infinite altitude, while wider cells do collapse and exhibit a self-sustained imbibition process. In the first case the liquid front reaches an equilibrium but is distorted, rising more at the center of the cell than close to the spacers. In fig. 5, we show the imbibition dynamics for cells with $e_0 = 500\,\mu\mathrm{m}$ and $w = 15\,\mathrm{mm}$ but membranes with different thicknesses (*i.e.* different bending stiffnesses B). We also report the maximum height h_m of the imbibition front as a function of the width w of the cell. Starting from the Jurin height h_e, h_m increases sharply as w approaches $2L^*$ (inset in fig. 5). Indeed, the capillary pressure tends to bend the flexible plate, which leads to smaller gap e_m between the plates and thus to a greater pressure. In terms of scalings, the typical torque per unit height exerted by the fluid on the flexible plate reads $w^2\gamma/e_m$ and equilibrates the resisting torque from the plate $B(e_0 - e_m)/w^2$. Within the limit of small perturbations, $e_m = e_0(1-\epsilon)$, this torque balance leads to $\epsilon \sim 1/[(2L^*/w)^4 - 1]$ and the maximum height is finally given by $h_m = 2\gamma/\rho g e_0(1-(w/2L^*)^4)$. Although our derivation is in principle restricted to small perturbations, this prediction is in good agreement with our experimental results (inset of fig. 5). We also note that the "flexible cells" region defined in fig. 4(b) can be further separated in two regions. Indeed, it is observed that capillary rise spontaneously starts in the thinnest cells. In thicker cells, though they do fulfill the criterion $w > 2L^*$, the walls are initially too far apart to interact through the liquid meniscii separating them. This situation typically occurs when e_0 is large in comparison with the capillary length $l_c = \sqrt{\gamma/\rho g}$. However, the collapse of the cell can be forced by pressing on the flexible sheet. Once triggered, the rise continues indefinitely.

Assuming the independence of the section of the cell with the height is valid far below the tip of the liquid front. However, far above the wetting front, the upper part of the flexible wall is expected to recover its original flat shape. In the vicinity of the liquid boundary, the (lower) bent and (upper) flat parts of the wall are connected by a transition region in which the membrane undergoes some stretching [28,29]. The persistent length along which the curvature of a pinched ribbon decays to zero is set by the balance of stretching and bending energies. This balance is given by $\ell_p \sim W^2/R^{1/2}\delta^{1/2}$ for a strip of width W and thickness δ with an imposed radius of curvature R at one

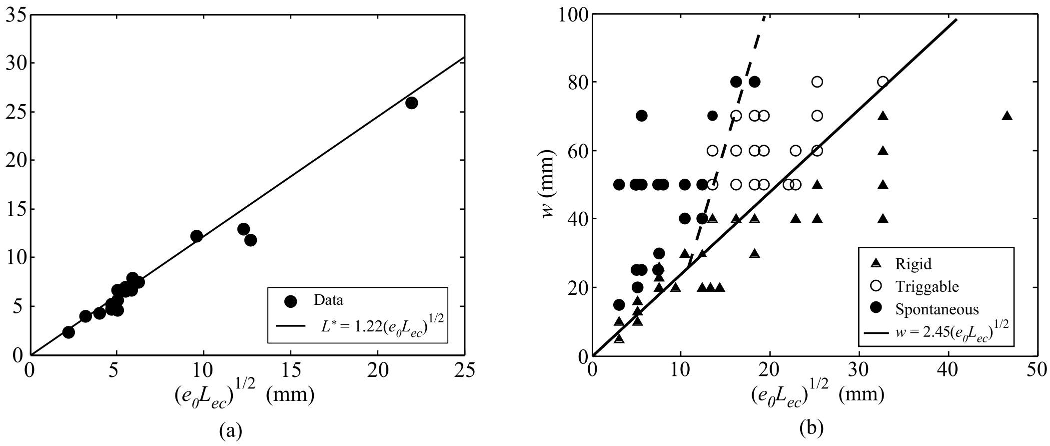

Fig. 4: (a) Width L^* of the dry region along the spacers as a function of $\sqrt{e_0 L_{ec}}$. Straight line: theoretical prediction $L^* = 1.22\sqrt{e_0 L_{ec}}$ (eq. (6)). (b) Possible imbibition modes as a function of the geometrical and physical properties of the system. Cells narrower than $2L^*$ do not enable the liquid to rise to infinity (triangles). Wider cells either show spontaneous imbibition (full dots) or need an initial triggering (open circles). The full line ($w = 2.45\sqrt{e_0 L_{ec}}$) separates elastic and rigid cells. Within the elastic domain, the dashed line separates spontaneous from triggered imbibition.

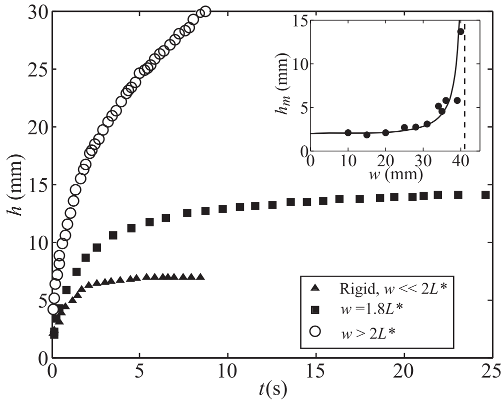

Fig. 5: $h(t)$ for cells of different thicknesses. If $w > 2L^*$ (circles), the cell is flexible enough to collapse and induce the infinite rise of the liquid. For $w \ll 2L^*$ (triangles), h saturates to h_e after a few seconds. If $w \lesssim 2L^*$ (squares), h still saturates, but the cell deforms moderately and the front reaches a higher position at a later time. Inset: the maximum height h_m of the front strongly increases as w approaches $2L^*$ (dashed line). The full line, of equation $h_m = 2\gamma/\rho g e_0(1 - (w/2L^*)^4)$, is a good fit to the experimental results.

end [28]. In the case of a flexible cell, the bent width is of the order of w and $R \sim w^2/e_0$, which leads to

$$\ell_p \sim w\sqrt{\frac{e_0}{\delta}}. \tag{7}$$

In the typical case of polypropylene sheets of thickness $\delta = 100\,\mu$m, $w = 2$ cm and $e_0 = 1$ mm, we find $\ell_p \sim 5$ cm. This characteristic length likely plays a role in determining the shape of the rising liquid front close to its highest point.

Dynamics. – We now describe the dynamics of liquid rise in wide cells ($w > 2L^*$). The height of rise $h(t)$ is found to increase as $t^{1/3}$ within a wide range of viscosities as represented in fig. 6(a). For instance in the case of silicon oil of viscosity $\eta = 15.4$ mPa s and surface tension $\gamma = 21\,\mathrm{mN\,m^{-1}}$, the liquid front reaches 150 mm in 1000 s. The dynamics do not depend on the cell dimensions w and e_0, but the physical properties of the fluid play a role: the rise is slower for larger viscosities and faster for larger surface tensions.

As sketched in fig. 3(b), the liquid mainly flows in a self-constructing wedge whose vertex is localized at a distance L^* from the spacers. To rise to height h, it confines in a space of typical radius $r \sim \gamma/\rho g h$ for capillary forces to balance gravity. The time for liquid to rise up to h in a capillary of size $\gamma/\rho g h$ is given by eq. (3) which expresses the characteristic time of capillary rise in a cylindrical tube as a function of the equilibrium Jurin height h_e. Applying this relationship locally and inverting it, we thus expect the height of the tip of the finger to follow

$$h(t) \sim \left(\frac{\gamma^2}{\eta\rho g}\right)^{1/3} t^{1/3}, \tag{8}$$

as predicted theoretically by Tang and Tang [30] and observed experimentally in several corner geometries by Ponomarenko *et al.* [22]. This result is in good agreement with our experimental observations since our data is well described over several decades in time by $\tilde{h}(t) = t^{1/3}$, with $\tilde{h} = h\left(\eta\rho g/\gamma^2\right)^{1/3}$ (fig. 6(b)).

However, we observe deviations from the prediction of eq. (8) at short and long times. At early times, we note that $h(t)$ increases faster than predicted by eq. (8). Indeed, cell deformations are initially weak and the wicking process should be described by the classical Washburn dynamics in a rigid cell of thickness e_0: $h(t) = \sqrt{\gamma e_0 t/\eta}$. Significant deformations of the cell only arise once h is large enough for the negative capillary pressure

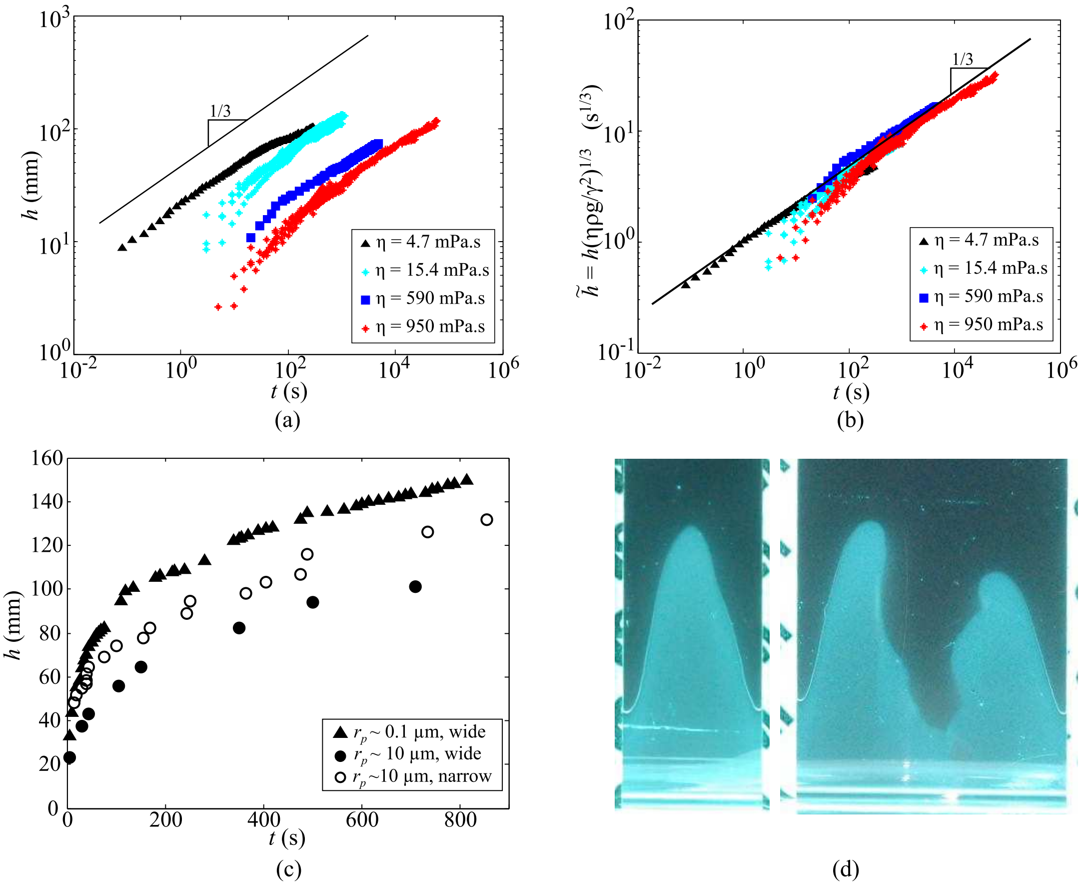

Fig. 6: (Colour on-line) (a) Height of the front as a function of time for silicon oils of viscosity spanning from 5 to 1000 mPa s. (b) Reduced height $\tilde{h}$ as a function of time. All data collapse on a single master curve $\tilde{h} = t^{1/3}$ (eq. (8)). The full line ($\tilde{h} \simeq t^{1/3}$) is a fit to the data of Ponomarenko *et al.* [22] for the capillary rise in a corner, which describes our data as well. (c) The imbibition front rises faster between smooth walls compared to rough walls. This effect is enhanced in wide cells, where there is more volume available for liquid in the central part of the cell. (d) In narrow cells (left, $w = 25$ mm), a single finger develops, whereas in wide cells (right, $w = 50$ mm) the front rises in two simultaneous fingers close to the spacers. Indeed, in this latter case the central region fills slower since the liquid is driven horizontally from the liquid corners.

to bend the flexible wall. As in the previous estimate of the height of the front, the typical torque induced by capillarity is given by $w^2 h\gamma/e_0$, where h is the front height. This torque balances the resistance of the plate which is bent along a typical distance ℓ_p. As the cell collapses, the curvature of the flexible plate reads e_0/w^2 and the corresponding torque is given by $\ell_p B e_0/w^2$. Capillary forces are finally expected to overcome bending stiffness as h becomes larger than

$$h^* \sim \frac{E(e_0\delta)^{5/2}}{\gamma w^3}. \tag{9}$$

We expect to recover the dynamics predicted by eq. (8) above h^*. Typical values of the relevant parameters ($E = 2$ GPa, $e_0 = 1$ mm, $\delta = 100\,\mu$m, $w = 2$ cm, $\gamma = 20$ mN/m) yield $h^* \sim 3$ cm, in qualitative agreement with experiments (fig. 6(a)).

At long times, we observe a slight deceleration of the liquid front (in comparison with the $\tilde{h}(t) \simeq t^{1/3}$ law). We believe that this effect is due to the horizontal drainage of the liquid from the wedges to the center of the cell as a consequence of the residual gap between the rigid and elastic plates. Indeed, experiments carried out with sheets of roughnesses on the order of $0.1\,\mu$m and $10\,\mu$m (as estimated by optical profilometry) show a more pronounced deceleration with the rougher plates (fig. 6(c)). For a given roughness, the rise is faster in narrower cells (smaller w), which suggests that a fast saturation of the central region reduces the drainage from the wedges.

Horizontal imbibition toward the center of the cell is finally responsible for some variation in the shape of the wicking front. In narrow cells ($w \gtrsim 2L^*$), a single wicking finger usually rises in the middle of the cell (fig. 6(d)). Yet, if the width of the cell is large, a pair of fingers develops close to the spacers, while the central region, away from the corners, fills through the horizontal drainage of the lateral fingers. In terms of dynamics law, we expect the horizontal imbibition to be described by a Washburn law in a porous medium with a typical pore size r_p given by the roughness of the plates: $x(t) \sim \sqrt{\gamma r_p t/\eta}$. The dynamics of the rising fingers $\tilde{h} \simeq t^{1/3}$) are initially faster than the lateral wicking, but slow down more rapidly. The pair of fingers formed in wide cells eventually merge at the center of the cell and form a single finger. In the case $w \gg 2L^*$, horizontal wicking from the fingers to the center takes a time $\tau_w \sim \eta w^2/\gamma r_p$. Using eq. (8), we thus find the height reached by the liquid as the fingers merge

$$h \sim \left(\frac{\gamma w^2}{\rho g r_p}\right)^{1/3}, \qquad (10)$$

which is independent of the liquid viscosity. In the typical case illustrated in fig. 6(d) with $w \simeq 5\,\text{cm}$ and $r_p \simeq 1\,\mu\text{m}$, we expect the fingers to merge for a height of the order of 17 cm, in fair agreement with the experimental observations.

Conclusion. – We have used a model elastic porous medium to show the peculiar imbibition mechanisms linked to capillary-induced deformations. We have demonstrated experimentally that deformability may be used to rise liquid through capillary imbibition up to infinite altitudes. In particular, we have shown that elastic and geometric properties of the cell dictate the mode of imbibition: slight deformations and Washburn law for the rise ($h \propto t^{1/2}$), or collapse of the cell wall and wedge-rise dynamics ($h \propto t^{1/3}$). In the latter case, the collapse may not occur spontaneously but can be triggered by the operator, which could be interesting for engineering applications. We expect these results to be relevant for more complex porous media ranging from flexible microfluidics channels to simplified versions of lung airways. However wicking through actual three-dimensional elastic material such as a solid foam or sponge may yield interesting results. Besides bending stiffness of the wall and capillary forces as in our model experiment, stretching of the whole matrix may then play a major role. Situations involving the erosion of the porous medium are finally of practical interest: while it rises in sugar, coffee also dissolves the matrix in which it is wicking.

* * *

We thank C. Duprat, B. Roman and D. Vella for fruitful discussions. This work was partially funded by the French ANR Mecawet.

REFERENCES

[1] Powers S. E. and Tambling M. E., *J. Contam. Hydrol.*, **19** (1995) 105.
[2] Morrow N. R. and Mason G., *Curr. Opin. Colloid Interface Science*, **6** (2001) 321.
[3] Ceballos-Ruano J. S., Kupka T., Nicoll D. W., Benson J. W., Ioannidis M. A., Hansson C. and Pintarb M. M., *J. Appl. Phys.*, **91** (2002) 6588.
[4] Alava M. and Niskanen K., *Rep. Prog. Phys.*, **69** (2006) 669.
[5] Saguy I. S., Marabi A. and Wallach R., *Trends Food Sci. Technol.*, **16** (2005) 495.
[6] Tanaka T., Morigami M. and Atoda N., *Jpn. J. Appl. Phys.*, **32** (1993) 6059.
[7] Prakash M., Quéré D. and Bush J. W., *Science*, **320** (2008) 931.
[8] Holbrook N. M. and Zwieniecki M. A., *Phys. Today*, **61**, issue No. 1 (2008) 76.
[9] de Gennes P. G., Brochard-Wyart F. and Quéré D., *Capillarity and Wetting Phenomena: Drops, Bubbles, Pearls, Waves* (Springer, New York) 2004.
[10] de Laplace P.-S., *Traité de mécanique céleste,* Livre Dixième (Imprimerie Royale, Paris) 1845.
[11] Bell J. M. and Cameron F. K., *J. Phys. Chem.*, **10** (1906) 658.
[12] Lucas V. R., *Kolloid-Z.*, **23** (1918) 15.
[13] Washburn E., *Phys. Rev.*, **17** (1921) 273.
[14] Quéré D., *Europhys. Lett.*, **39** (1997) 533.
[15] van Honschoten J. W., Escalante M., Tas N. R., Jansen H. V. and Elwenspoek M., *J. Appl. Phys.*, **101** (2007) 094310.
[16] van Honschoten J. W., Escalante M., Tas N. R. and Elwenspoek M., *J. Colloid Interface Sci.*, **329** (2009) 133.
[17] Tas N. R., Escalante M., van Honschoten J. W., Jansen H. V. and Elwenspoek M., *Langmuir*, **26** (2010) 1473.
[18] Yang Y., Gao Y. F., Sun D. Y., Asta M. and Hoyt J. J., *Phys. Rev. B*, **81** (2010) 241407(R).
[19] Halpern D. and Grotberg J. B., *J. Fluid Mech.*, **244** (1992) 615.
[20] Heil M. and White J. P., *J. Fluid Mech.*, **462** (2002) 79.
[21] Hazel A. L. and Heil M., *Proc. R. Soc. London, Ser. A*, **461** (2005) 1847.
[22] Ponomarenko A., Quéré D. and Clanet D., *J. Fluid Mech.*, **666** (2011) 146.
[23] Bico J., Roman B., Moulin L. and Boudaoud A., *Nature*, **432** (2004) 690.
[24] Duprat C., Aristoff J. M. and Stone H. A., `http://arxiv.org/abs/1008.3702` (2011).
[25] Aristoff J. M., Duprat C. and Stone H. A., *Int. J. Non-Linear Mech.*, **46** (2011) 648.
[26] Maurel A., Cobelli P., Pagneux V. and Petitjeans P., *Appl. Opt.*, **48** (2009) 380.
[27] Roman B. and Bico J., *J. Phys.: Condens. Matter*, **22** (2010) 493101.
[28] Lobkovsky A. E. and Witten T. A., *Phys. Rev. E*, **55** (1997) 1577.
[29] Mahadevan L., Vaziri A. and Das M., *EPL*, **77** (2007) 40003.
[30] Tang L.-H. and Tang Y., *J. Phys. II*, **4** (1994) 881.